Supporting Information

Magnetoreception of Photoactivated Cryptochrome 1 in Electrochemistry and Electron Transfer

Zheng Zeng,[†] Jianjun Wei,[†] Yiyang Liu,[†] Wendi Zhang,[†] Taylor Mabe[†]*

[†]Department of Nanoscience, Joint School of Nanoscience and Nanoengineering (JSNN), University of North Carolina at Greensboro, 2907 E. Gate City Blvd, Greensboro, NC 27401, United States.

Corresponding Authors
j_wei@uncg.edu (j. Wei)

TABLE OF CONTENTS

SIMULATION METHOD SECTION

Electron transfer model for k^0

The electron transfer between an electroactive reporter such as cryptochrome 1 and an electrode can be written as follows by assuming the direct superexchange pathway is the dominant pathway.[S1]

$$CRY1^* \xrightarrow{k_{ox}} Electrode \quad \text{(S1)}$$

Note that here the acceptor is actually the electrode. A very important feature of electrochemistry is that the Gibbs free energy of the reaction above can be easily changed by the overpotential η, therefor the rate constant k_{ox} is also subject to the overpotential η. Therefore, in cyclic voltammetry, the crucial step is to get the expression of k_{ox} in terms of η by using a density of states (DOS) treatment and assuming a Marcus (Gaussian) density of states.

We assume that the DOS of the oxidized form is a normalized Gaussian distribution with $\sqrt{2\lambda k_B T}$ as the standard deviation, then

$$\rho(\varepsilon) = \frac{1}{\sqrt{4\pi\lambda k_B T}} \exp\left(-\frac{\left(\lambda + (\varepsilon_F - \varepsilon) + e\eta\right)^2}{4\lambda k_B T} \right) \quad \text{(S2)}$$

Where $\rho(\varepsilon)$ is the DOS of the electrode, λ is the reorganization energy, k_B is the Boltzmann's constant, T is temperature in Kelvin, ε_F is the Fermi energy, ε is the energy of an electronic state in the electrode, e is the elementary charge, and η is the overpotential. And the overall oxidation rate constant can be obtained by using Fermi's golden rule:

$$k_{ox} = \frac{2\pi}{\hbar}|H_{DA}|^2 \int_{-\infty}^{\infty} \rho(\varepsilon) f(\varepsilon) \cdot \rho(\varepsilon, \lambda) d\varepsilon = \frac{2\pi}{\hbar}|H_{DA}|^2 \frac{1}{\sqrt{4\pi\lambda k_B T}} \int_{-\infty}^{\infty} \rho(\varepsilon) f(\varepsilon) \exp\left(-\frac{\left(\lambda + (\varepsilon_F - \varepsilon) + e\eta\right)^2}{4\lambda k_B T} \right) d\varepsilon \quad \text{(S3)}$$

Where h is the Planck constant, H_{DA} is the effective electronic coupling between the electrode

and the probe states, *f(ε)* is Fermi function. Since η is a function of time *t* and scan rate *v*, the rate constants for oxidation k_{ox} depend on the time and scan rate.

To compare the intrinsic charge transfer properties of different systems, the standard heterogeneous rate constant k^0 is used:

$$k^0 = k_{ox}\left(\eta = 0\right) \tag{S4}$$

Hence the standard heterogeneous rate constant k^0 is given by

$$k^0 = \frac{2\pi}{\hbar}\left|H_{DA}\right|^2 \frac{1}{\sqrt{4\pi\lambda k_B T}} \int_{-\infty}^{\infty} \rho\left(\varepsilon\right) f\left(\varepsilon\right) \exp\left(-\frac{\left(\lambda + \left(\varepsilon_F - \varepsilon\right)\right)^2}{4\lambda k_B T} \right) d\varepsilon \tag{S5}$$

These calculations allow us to make plots of the Faradaic peak potential shift from formal potential versus *log(v)* for different k^0 values. Note that formal potential is the y-intercept at the scan rate of 0 V s^{-1} by plotting peak potential vs. scan rate. These calculated curves can then be compared to plots of the experimental Faradaic peak potential shift versus scan rates to extract the k^0 values for different systems.

SUPPLEMENTARY FIGURES AND TABLES SECTION

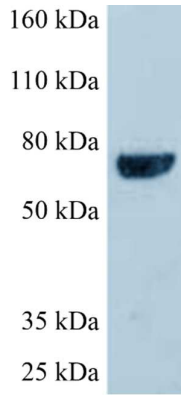

Figure S1. Polyacrylamide gel electrophoresis analysis of purified CRY1 with a molecular weight of 67 kDa.

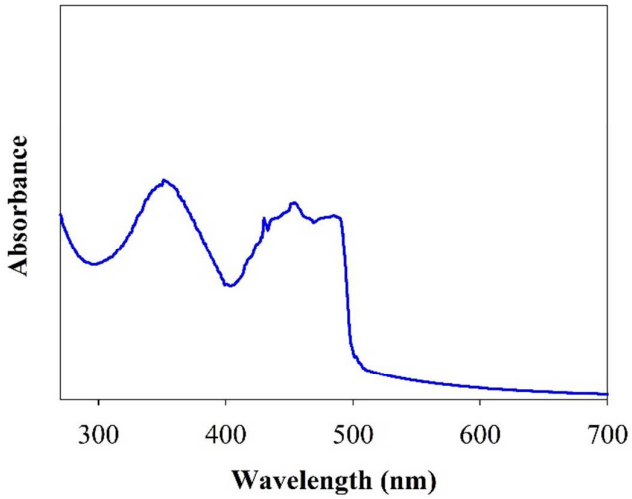

Figure S2 UV-Vis absorption spectrum of CRY1 performed in a solution of 50 mM Tris buffer containing 500 mM NaCl under pH=8, indicating its blue-light receptor role.[S2-S3]

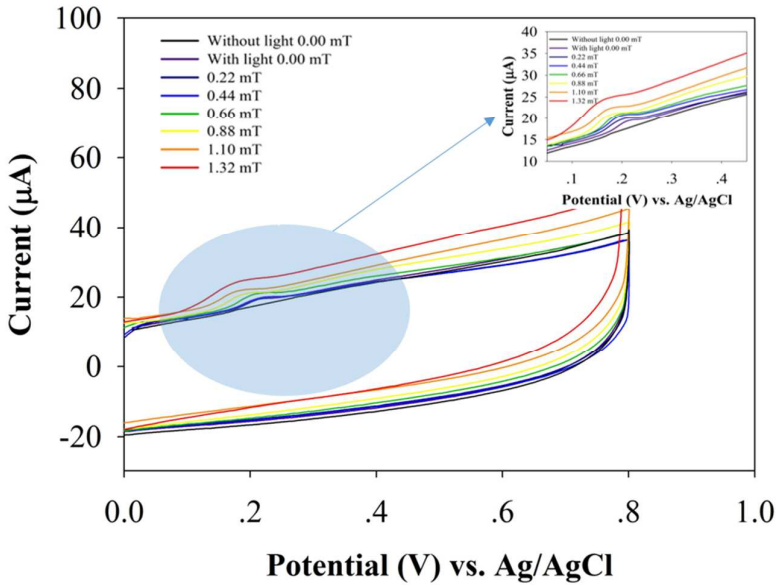

Figure S3. Cyclic voltammograms for the gold slide surface immobilized with CRY1 with/without blue light excitation in the absence of magnetic field and with blue light excitation under different magnetic fields at the scan rate of 4 V s^{-1}.

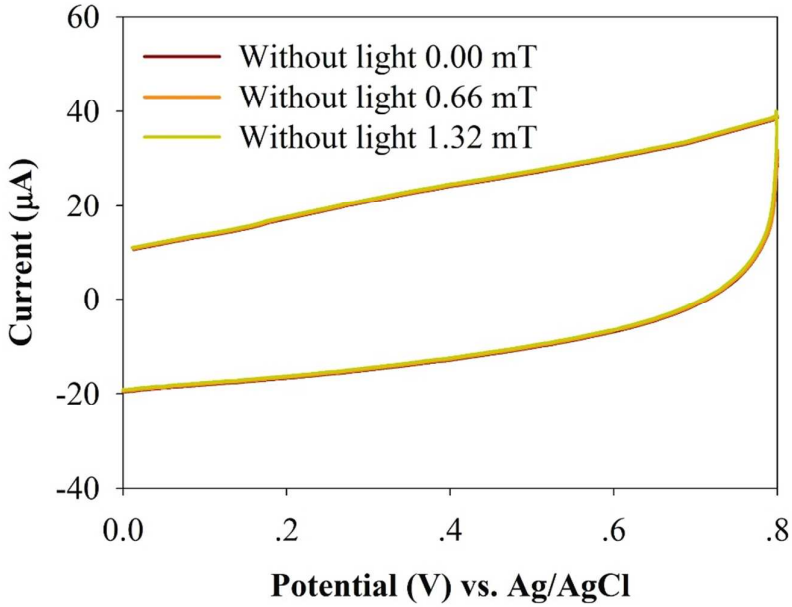

Figure S4 Cyclic voltammograms for the gold slide surface immobilized with CRY1 without blue light excitation under different magnetic fields at the scan rate of 4 V s^{-1}.

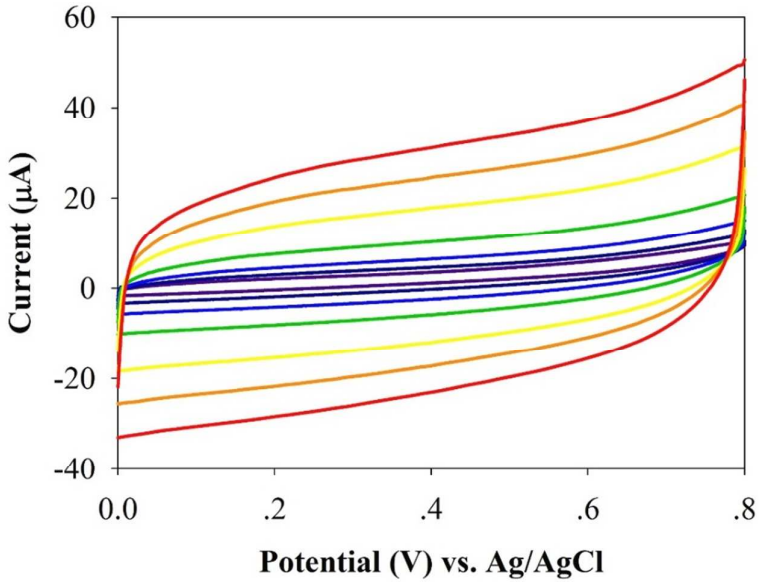

Figure S5 Cyclic voltammograms for the SAM/gold slide surface in which has not been immobilized with CRY1 with blue light excitation in the absence of an external magnetic field at the scan rate of 0.2 V s^{-1}, 0.5 V s^{-1}, 1 V s^{-1}, 2 V s^{-1}, 4 V s^{-1}, 6 V s^{-1}, and 8 V s^{-1}.

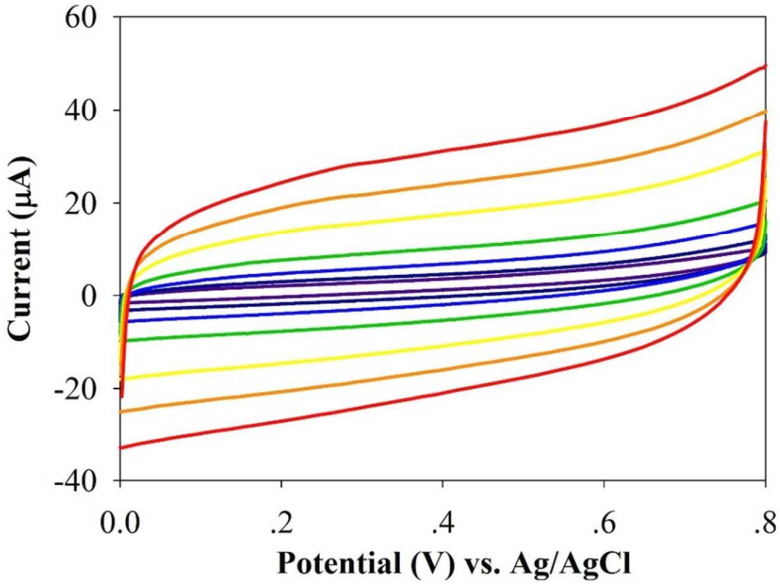

Figure S6 Cyclic voltammograms for the SAM/gold slide surface in which has not been immobilized with CRY1 with blue light excitation under 1.32 mT of magnetic field at the scan rate of 0.2 V s^{-1}, 0.5 V s^{-1}, 1 V s^{-1}, 2 V s^{-1}, 4 V s^{-1}, 6 V s^{-1}, and 8 V s^{-1}.

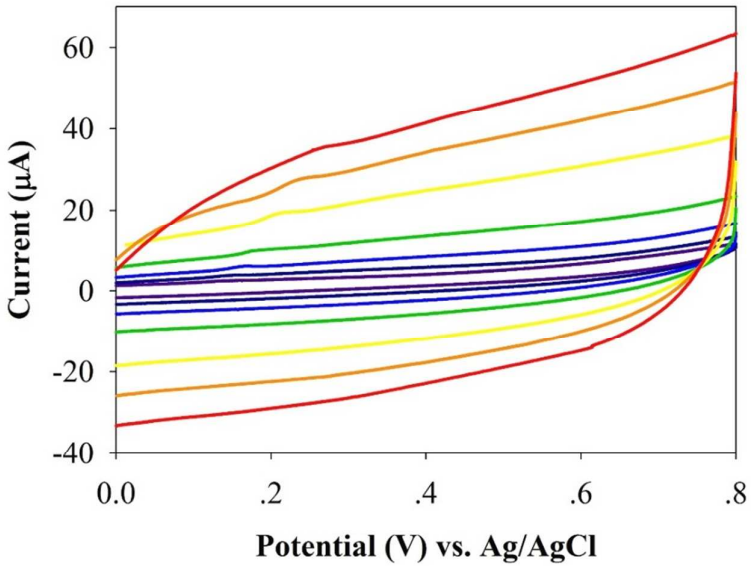

Figure S7 Cyclic voltammograms for the gold slide surface immobilized with CRY1 with blue light excitation in the absence of an external magnetic field at the scan rate of 0.2 V s^{-1}, 0.5 V s^{-1}, 1 V s^{-1}, 2 V s^{-1}, 4 V s^{-1}, 6 V s^{-1}, and 8 V s^{-1}.

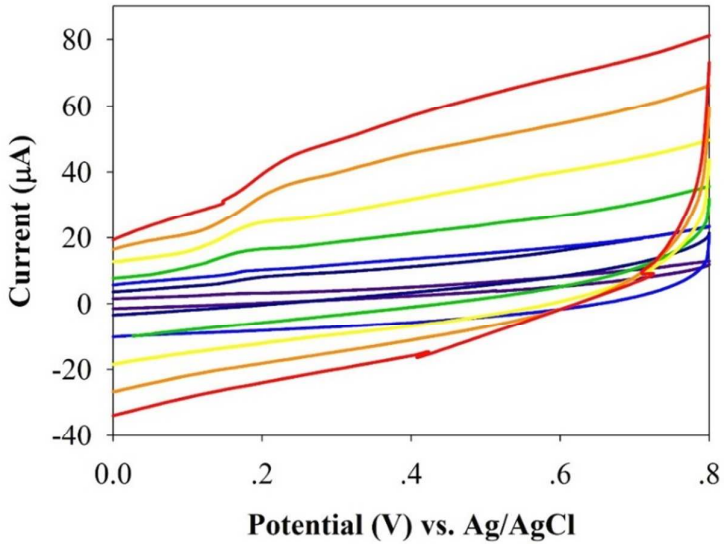

Figure S8 Cyclic voltammograms for the gold slide surface immobilized with CRY1 with blue light excitation under 1.32 mT of magnetic field at the scan rate of 0.2 V s^{-1}, 0.5 V s^{-1}, 1 V s^{-1}, 2 V s^{-1}, 4 V s^{-1}, 6 V s^{-1}, and 8 V s^{-1}.

Table S1 The dependence of the peak current on the voltage scan rate under different magnetic fields.

	Peak Current (μA)						
Scan Rate (V/s)	0.00 mT	0.22 mT	0.44 mT	0.66 mT	0.88 mT	1.10 mT	1.32 mT
0.2	0.1929	0.2195	0.2755	0.2812	0.3297	0.4611	0.5912
0.5	0.2946	0.3738	0.4304	0.5004	0.5956	0.7923	1.0261
1	0.4615	0.6332	0.7752	0.8749	0.9747	1.1971	1.4968
2	0.7551	0.9176	1.0802	1.4067	1.6537	1.9178	2.3322
4	1.4628	1.7877	2.1226	2.4283	2.7576	3.2334	3.7239
6	2.0840	2.6007	3.0236	3.4965	4.0614	4.7258	5.2398
8	2.6518	3.3525	3.9135	4.4291	5.0483	6.0389	6.6106

Table S2 The dependence of the peak potential on the scan rate under different magnetic fields

	Peak Potential Shift (V)						
Scan Rate V/s	0.00 mT	0.22 mT	0.44 mT	0.66 mT	0.88 mT	1.10 mT	1.32 mT
0.2	0.0211	0.0172	0.0151	0.0127	0.0098	0.0077	0.0064
0.5	0.0286	0.0224	0.0203	0.0178	0.0150	0.0131	0.0101
1	0.0414	0.0299	0.0280	0.0254	0.0201	0.0183	0.0167
2	0.0558	0.0482	0.0456	0.0356	0.0325	0.0271	0.0250
4	0.0836	0.0733	0.0682	0.0634	0.0454	0.0439	0.0379
6	0.1116	0.1032	0.0948	0.0863	0.0708	0.0565	0.0482
8	0.1370	0.1188	0.1092	0.1014	0.0914	0.0733	0.0601

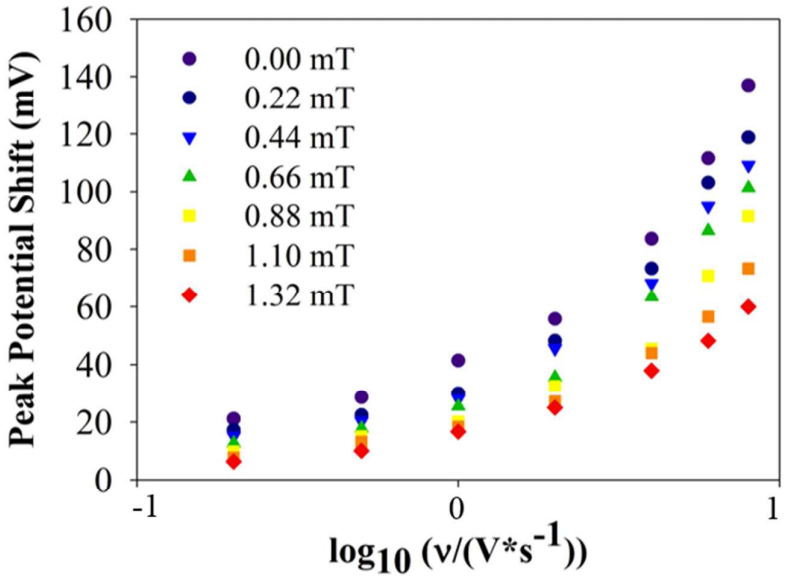

Figure S9 The dependence of the peak potential on the scan rate under different magnetic fields.

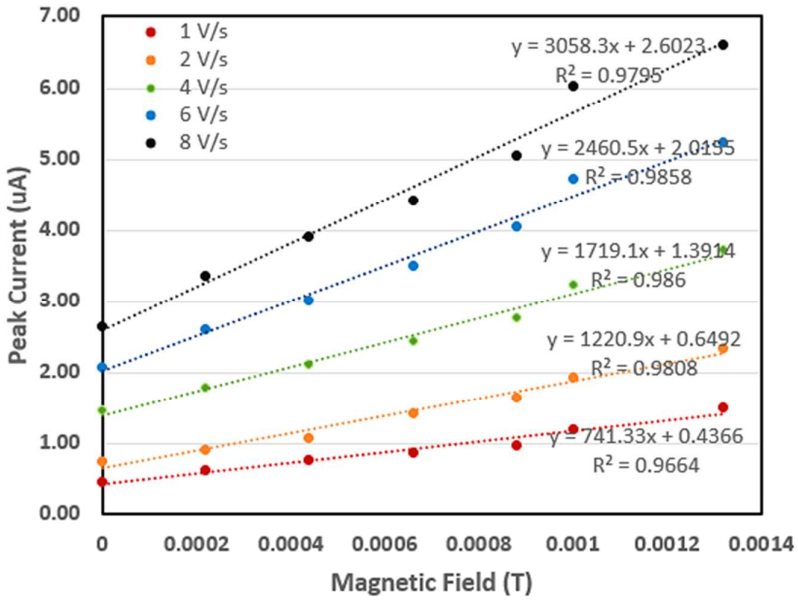

Figure S10. Peak current vs. magnetic field at different cyclic voltammetry scan rates.

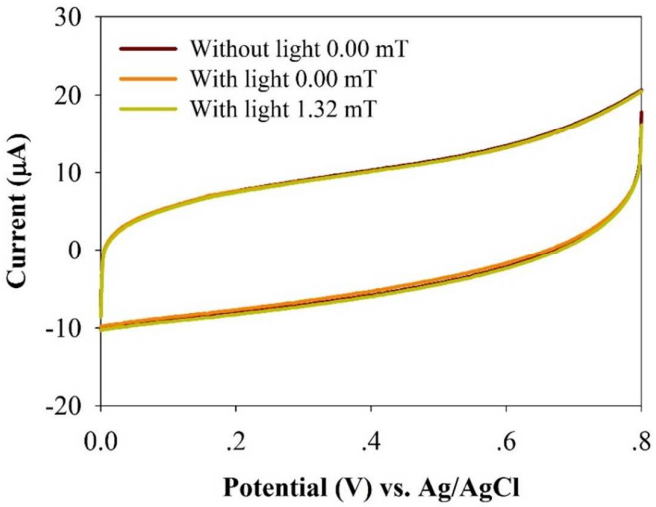

Figure S11. Cyclic voltammograms at positive voltage for the gold slide surface immobilized with an empty vector negative control with/without blue light excitation in the absence of magnetic field and with blue light excitation in the presence of magnetic fields at the scan rate of 4 Vs^{-1}.

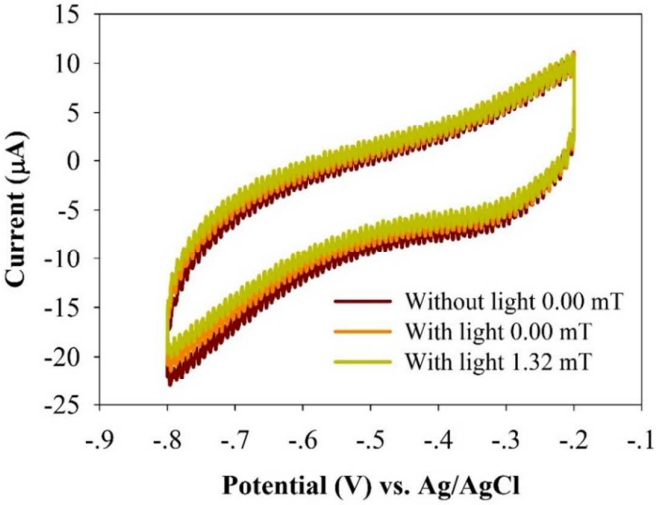

Figure S12. Cyclic voltammograms at negative voltage for the gold slide surface immobilized with an empty vector negative control with/without blue light excitation in the absence of magnetic field and with blue light excitation in the presence of magnetic fields at the scan rate of 4 Vs^{-1}.

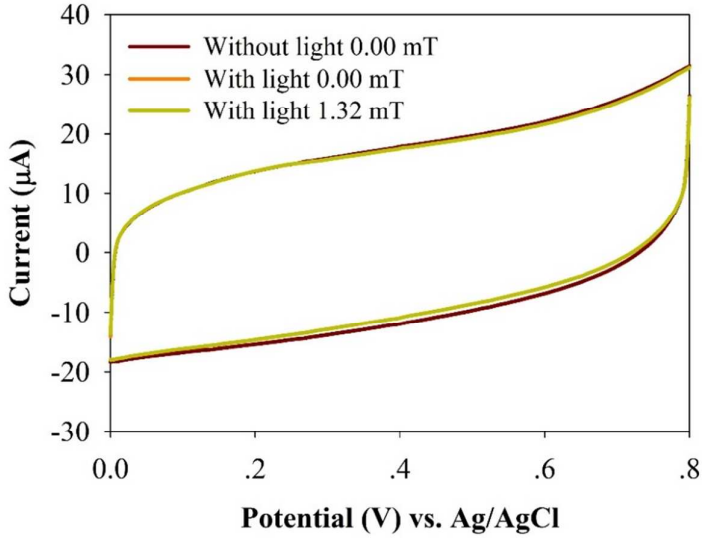

Figure S13. Cyclic voltammograms at positive voltage window for the gold slide surface immobilized with FAD with/without blue light excitation in the absence of magnetic field and with blue light excitation in the presence of magnetic fields at the scan rate of 4 V s^{-1}.

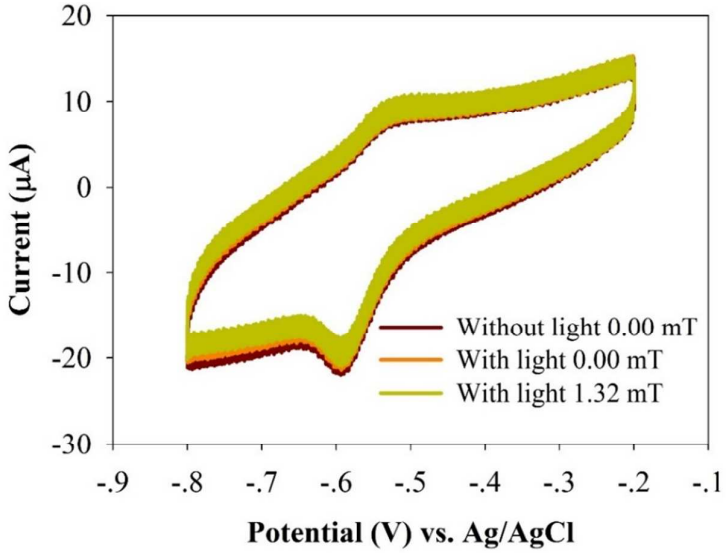

Figure S14. Cyclic voltammograms at negative voltage window for the gold slide surface immobilized with FAD with/without blue light excitation in the absence of magnetic field and with blue light excitation in the presence of magnetic fields at the scan rate of 4 Vs^{-1}.

SUPPORTING REFERNCES

S1. Xing, Y. (2015). *Theoretical and Experimental Explorations of Charge Transfer in Small Molecules and Peptide Nucleic Acids* (Doctoral dissertation, University of Pittsburgh).

S2. Kottke, T., Batschauer, A., Ahmad, M., & Heberle, J. Blue-light-induced changes in Arabidopsis cryptochrome 1 probed by FTIR difference spectroscopy. *Biochem.*, **2006**, *45*(8), 2472-2479.

S3. Kutta, R. J., Archipowa, N., Johannissen, L. O., Jones, A. R., Scrutton, N. S., Vertebrate Cryptochromes are Vestigial Flavoproteins, *Sci. Rep.*, **2017**, 7, 44906